



## Design and control of grid interfaced voltage source inverter with output LCL filter

Sajad Sarajian<sup>1,\*</sup> and Mahmoud Ranjbar<sup>2</sup>

<sup>1</sup>Islamic Azad University, Ashtian Branch, Ashtian Iran.

<sup>2</sup>Powerelectronics Department, Niroo Research Institute, Tehran, Iran.

### ARTICLE INFO

#### Article history:

Received: 19 February 2014;

Received in revised form:

19 June 2014;

Accepted: 29 June 2014;

#### Keywords

Voltage source inverter (vsi),  
Grid-interfaced converter,  
Filters design,  
Power electronics,  
Digital controller.

### ABSTRACT

This paper presents design and analysis of an LCL-based voltage source converter using for delivering power of a distributed generation source to power utility and local load. LCL filter in output of the converter analytically is designed and its different transfer functions are obtained for assessment on elimination of any probable parallel resonant in power system. The power converter uses a controller system to work on two modes of operation, stand-alone and grid-connected modes, and also has a seamless transfer between these two modes of operation. Furthermore, a fast semiconductor-based protection system is designed for the power converter. Performance of the designed grid interface converter is evaluated by using an 85-kVA industrial setup.

© 2014 Elixir All rights reserved

### Introduction

DISTRIBUTED Generation systems such as microturbines, fuel cells, wind turbines and photovoltaic systems are expected to represent a large portion of power generation capacity, especially in future [1]. In particular, MTG is witnessed to be capable of delivering clean energy from a wide variety of fuels with superior safety and low emissions. The capacity of MTG can be ranged from several kilowatts up to megawatts. As it is often sited dispersedly near the industrial load, it is deemed as a category of distributed generations nowadays [2–9]. A direct merit exhibited by such electric power generation is to provide the utility a way to defer power plant construction, while offering customers a clean resource at reasonable cost.

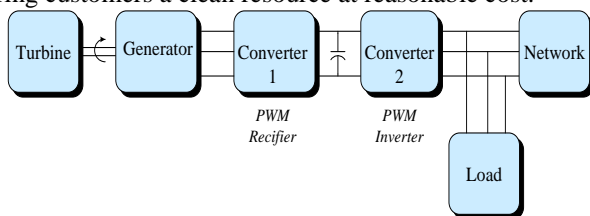


**Figure 1. Block diagram of power electronic interface configuration for a MT**

There are essentially two types of micro turbine designs. One is a split shaft design that uses a power turbine rotating at 3600 rpm and a conventional generator (usually induction generator) connected via a gearbox. The power inverters are not needed in this design. Another is a high-speed single-shaft design with the compressor and turbine mounted on the same shaft as the PM synchronous generator. The advantages of the high-speed permanent-magnet generator are its compact size, low-mass design and the elimination of the gearbox, resulting in reduction and simplification of the generating package. The use of power electronics enhances the system performance because of the asynchronous operation of the gas turbine, with the gas turbine speed independent of the grid frequency. It enables the

gas turbine speed control to adjust for optimal gas turbine efficiency [10-14].

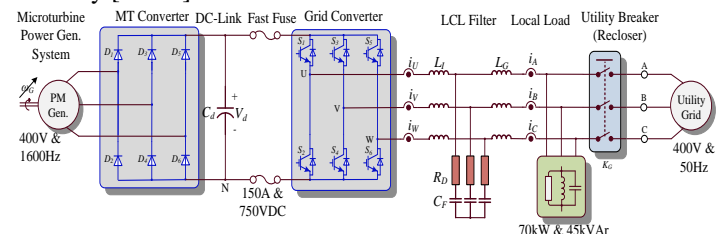


**Figure 2. General configuration of constructed grid-tied inverter**

A general view of microturbine system is shown in Fig. 1. The configuration of an MTG system is composed of a gas turbine, a compressor, and an AC generator. They are inertia welded on a single shaft to simplify the mechanical structure. When this shaft turns at the speed of the turbine, the generator would provide high-frequency AC electricity that requires a rectifier (Converter 1 in Fig. 1) and an inverter (Converter 2 in Fig. 1) to interface with utility network. By employing different control strategies, the MTG can operate as a power conditioner for the grid-connected operation to improve the quality of supplying power or sever from the grid as an emergency generator [15], [16].

The grid-connected inverter in MT's power electronic interface should operate in grid-tied and off-grid modes in order to provide power to the emergency load during system outages. Moreover, the transition between the two modes should be seamless to minimize any sudden voltage change across the emergency load or any sudden current change to the grid. A seamless transfer between both modes has been proposed in [17]. However, the grid current controller and the output voltage controller must be switched between the two modes, so the outputs of both controllers may not be equal during the transfer instant, which will cause the current or voltage spikes during the switching process. On the other hand, as the grid-interactive inverter should operate in off-grid mode, the filter capacitor is

necessary. Nevertheless, the filter capacitor current affects the waveform quality of the grid current in polluted grid, especially at low output power [18].

This paper deals with design and construction of a three-phase 85-kVA grid-interactive inverter and its DSP-based digital controller. Two different control modes are considered for the inverter: stand-alone control mode, and grid-connected control mode. Furthermore the inverter controller is expected to have a soft and seamless transfer between these two control modes. In the following sections, first the overall configuration of system is discussed in section II, and then in section III, the controller of inverter is described; a protection system proper for the power inverter is presented in section IV; section V shows the experimental results of the implemented inverter; paper's conclusion is also presented in section VII.

### THREE-PHASE GRID-INTERACTIVE INVERTER

Power configuration of the developed system is depicted in Fig. 2. It consists of a primary power source, a full bridge diode rectifier, a DC-link, a full bridge grid converter with  $LC$  filter, a power electromechanical relay  $K$ , and the three-phase 400-V/50-Hz grid. The primary power source is, in fact, a microturbine generator that in this study is replaced with a grid connected power autotransformer. The parameters used in the constructed system are shown in Table I.

TABLE I: System Parameters

| Parameter                              | Value                            |
|--|----------------------------------|
| System voltage: $V_{L-L} (=V_b)$       | 400 $V_{rms}$                    |
| Fundamental frequency: $f_{Line}$      | 50 Hz                            |
| Load rated $P_n, Q_n, S_n (=S_b)$      | 70 kW, 45 kVAr, 85 kVA           |
| Dc link voltage: $V_{dc}$              | 760 Vdc (1.9 pu)                 |
| DC-link Capacitor, $C_{dc}$            | 4200 $\mu F$                     |
| Switching Frequency                    | 2 kHz (40 pu)                    |
| Sampling Frequency                     | 4 kHz (80 pu)                    |
| PI controller                          | $K_p=0.5, K_I=200$               |
| Load Power Factor                      | 0.85                             |
| System impedance arameters: $L_s, R_s$ | 55 $\mu H, 2.5 m\Omega$          |
| LCL filter parameters                  |                                  |
| $L_1, R_1$                             | 0.83 mH (13.85%), 52 $m\Omega$   |
| $L_2, R_2$                             | 0.75 mH (12.52%), 12 $m\Omega$   |
| $C_F$                                  | 270 $\mu F$ (15.97%)             |
| $R_d$                                  | 0.6 $\Omega$ (31.88%)            |
| $f_{res}$                              | 488 Hz (9.76 $f_{Line}=9.76$ pu) |

### DIGITAL CONTROLLER OF INVERTER

A control technique should be designed for inverter (750 V-DC/ 400 V-AC (L-L), rated 70 kW) to satisfy following performance characteristics:

- 1)Low load regulation (less than 5%): the AC output voltage of the DG system should be maintained at 400 V (L-L)/230 V (L-N) independent of load conditions,
- 2)Minimum THD: DG system when feeding to the nonlinear loads, such as rectifiers, SMPS, must generate minimum harmonics currents and voltages in compliant with IEEE 519 std,
- 3)Fast transient response: system must be able to produce output AC voltage with minimum overshoot or undershoot,
- 4)Short circuit protection: system must be able to provide protection from excessive overload conditions,
- 5)Different control modes: the microturbine grid converter should operate in both grid-connected control mode and stand-alone control mode,
- 6)A soft and seamless transfer between different control modes: in transition from one control mode to the other, amplitude and frequency of the voltage at the PCC must not exit its limitation ( $V_{rated} \pm 10\%$  &  $f \pm 2$  Hz),

7)Anti-islanding detection capability: based on IEEE 1547 std [19], all DGs must be disconnected from an islanded grid in a specified time,

8)Paralleling capability: in order to increase the reliability of power source converter, it should operate in parallel with other converters, especially in stand-alone operation mode,

9)Deals with distorted and/or unbalanced grid voltage: grid voltage is commonly distorted and/or unbalanced. Therefore, it causes grid-tied inverters to inject a distorted and/or unbalanced current to the power system. So, inverter's controller must be able to suppress these harmonic effects.

10) Decoupled P & Q control for grid-connected inverter: in grid-connected control mode the control of the active and reactive power must be decoupled from each other.

### Island Mode Operation

One of the most uses of microturbine system is in places that are far from electric utility power system [20]. In this case, this device should produce a power appropriate for local load which is supplied by microturbine system. Therefore, system must be controlled in such a way that reference voltage appears in output terminal and delivers power to the local loads [21].

In stand-alone control mode, no grid exists so the output voltages need to be controlled in terms of amplitude and frequency and thus the reactive and, respectively, active power flow is controlled [22-24]. In the case of unbalance between the microturbine generated and the load required power, adjustment of the speed of the microturbine can regulate the produced power in a limited range. The potential excess of power will be quickly dissipated in a damp resistor by starting a chopper control located in DC-link of inverter (it does not show in Fig. 2). One of the common control methods of inverter, in this case, is control of output voltage in dq plan. The control structure for stand-alone control mode is shown in Fig. 3 and it consists of output voltage controller, and current limiter. The output voltage controller is aiming to control the output voltage with a minimal influence from the shape of the nonlinear load currents or load transients. A standard PI controller operating in the synchronously rotating coordinate system where is kept to zero is used. As it can be seen form Fig. 3, at first, the output voltages are measured (by voltage sensors) and after converting to  $V_d$  and  $V_q$ , they are subtracted from their references, and the resultant error signals send to two separate PI controllers; PI controllers produce the pattern voltages for switching in dq plan. Then, these voltages are converted to the pattern voltage in abc plan and introduce to PWM generating block. Finally, the PWM generating block generates 6 PWM pulses for IGBT switches in inverter. When the load current exceeds the rated current, the current limiter will decrease the output voltage reference in the allowed range, and for fast response there is a direct forward connection to the voltage controller output. This situation can occur if at a certain load, the generated power decreases due to lower microturbine input fuel or during overloading.

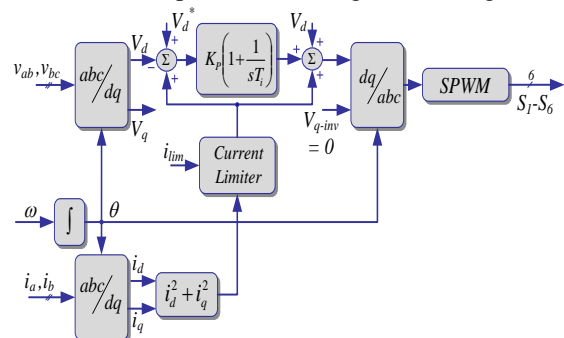


Figure 3. Block diagram of stand-alone control of inverter.

**Grid-Tied Mode Operation**

In grid-connected control mode, principally all the available power that can be obtained from the microturbine is delivered to the grid. Moreover, compensation of reactive power is possible if required. The block diagram of control arrangement for grid-connected control mode is demonstrated in Fig. 4. Standard *PI*-controllers are used to adjust the grid currents in the *dq*-synchronous frame. A decoupling of the cross-coupling is implemented in order to compensate the couplings due to the output filter [12]. In order to achieve a zero phase angle between voltage and current, the reference current in the *q*-axis,  $I_q^*$ , of the current loop is in general set to zero and so unity power factor can be achieved.

In grid connected control mode, the controller works as current controller. It sets the voltage reference for a standard sinusoidal modulation (SPWM) that generates pulses for the switches of the grid converter via a shielded cable link. A PLL is designed to make the inverter synchronism with grid. Also, the reference currents in *dq*-axis,  $I_d^*$  and  $I_q^*$ , can be drawn from the following relations:

$$p = v_d i_d + v_q i_q \xrightarrow{v_q=0} i_d^* = \frac{p^*}{v_d} \tag{1}$$

$$q = v_d i_q - v_q i_d \xrightarrow{v_q=0} i_q^* = \frac{q^*}{v_d} \tag{2}$$

where  $v_d$  and  $v_q$  are the grid voltage in *dq*-axis, and  $p^*$  and  $q^*$  are reference active and reactive power that inverter is expected to deliver to the grid.

Furthermore, current feedback Proportional Integrate (PI) control with grid voltage feed-forward is commonly used in stationary reference frame for current-controlled inverters. But these solutions have two main drawbacks: inability of the PI controller to track a sinusoidal reference without steady-state error and poor disturbance rejection capability. This is due to the definite control loop gain required for system stability at the *LCL*-filter resonance frequency.

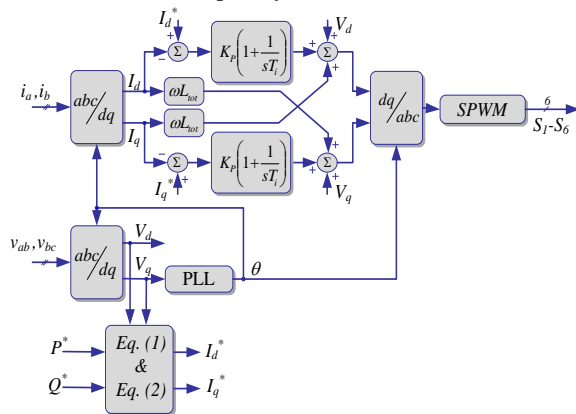


**Figure 4. Block diagram of grid-connected inverter control mode.**

Grid voltage feed-forward is often used to get a good dynamic response, but this leads in turn to the increase of the grid-voltage background harmonics in the current waveform because of the imperfect compensations [25], [26].

**Seamless Transfer**

In order to realize the seamless transfer between grid-tied and off-grid modes, the load voltage must match the magnitude, frequency, and phase of the grid voltage well before connecting to the utility. The load voltage can match the grid voltage well through sampling the grid voltage as the reference voltage before connecting to the grid, especially in polluted grid voltage. The detailed process of the seamless transfer between the two modes is illustrated in the following.

Off-grid mode to grid-tied mode:

- I. Detect that the grid is normally operating.
- II. Adjust the inverter’s output voltage (or load voltage) to match the magnitude and phase of the grid voltage.
- III. Once the load voltage is equal to the grid voltage, turn on the relay *K* and switch inverter from voltage-controlled mode to current-controlled mode, with the reference current being equal to the load current.
- IV. Change the reference current slowly to the desired current (both magnitude and phase).

**Grid-tied mode to off-grid mode:**

- I. Detect a fault on the grid and give a turn off signal to the relay *K*. **Monitor the magnitude and phase of the load voltage.**
- II. When the relay current goes to zero, transit the inverter to a voltage-controlled mode, with the voltage reference being derived from the load voltage.
- III. Ramp up the magnitude of the load voltage from its initial value to the rated value.

**POWER CONVERTER’S PROTECTION SYSTEM**

Electrical faults, that can damage the power converter, are categorized in two groups: overvoltage and over-current. Each one of these faults has different severe effects on the system, so an effective protection method should be used.

**Over current**

Many reasons may cause an over-current occurrence in a power inverter. Overload and short-circuit are the main and common reasons of over-current fault in a power inverter. Overload fault lasts in a longer time (e.g. 1 min.) and current value is a few times of nominal current (e.g. 1-2 p.u). The delayed function fuses are used to protect system against this fault, while short circuit lasts for a short time (e.g. 10-μs to 1-ms) and current increases several times beyond rating current (e.g. 2-100 pu). As a result, the short-circuit fault is more severe than over-current and therefore needs a faster protection system.

Over current is the most common fault; it is implemented in both software and hardware. Semiconductor fuses and gate driver protection are used as hardware methods.

Phase to phase short circuit on inverter AC side (i.e. Fig. 5(a)) makes the biggest current flowing in IGBT switches; due to AC side filter inductors; current increasing rate is not too fast, as a result, both common software and hardware methods can do effective protection in this case.

Shout through at dc link (i.e. Fig. 5(b)) is another severe fault; it should note that shout through is not expected to happen after completing the control system and required protections; however if this fault happens, effective protection is not possible either by software or hardware. A brief analysis regarding shout through and AC side short circuit is explained as follows.

Considering 2 μH leakage inductance in dc link at experimental setup and 800 μH filter inductance at inverter AC side; current rising rate due to short circuit at dc link and AC side are 375 and 0.47 A/μS, respectively.

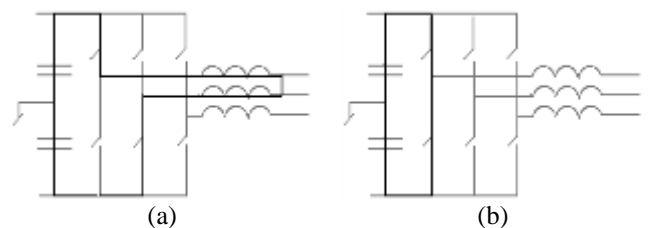


**Figure 5. Over current faults (a) shout through (b) AC side short circuit**

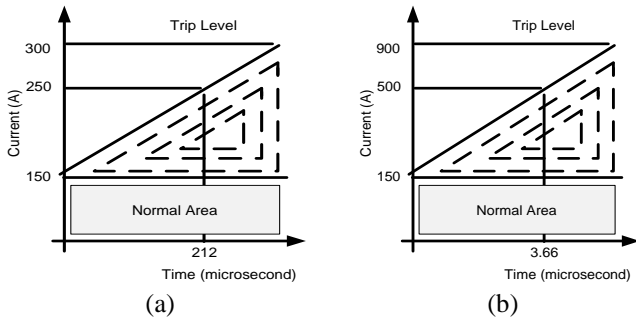


**Figure 6. Over current Protection criteria (a) inverter AC side (b) dc link**

It should note that dc link voltage at steady state is 750 V, subsequently current rise rate is as:

$$\frac{di}{dt} = \frac{V(V)}{L_{\sigma}(\mu H)} \frac{A}{\mu S} \quad (3)$$

Where  $L_{\sigma}$  is the leakage inductance and  $V$  is the dc link voltage. Finally, protection areas in dc link and inverter AC side are shown in Figs. 2(a) and (b), respectively. Shaded areas demonstrate the protection system setting points.

In the constructed inverter, following protection systems are considered to protect it against any probable over-current or short-circuit faults:

- 1) A software-based protection system implemented by DSP *digital controller*: it can clear the fault in less than 120- $\mu$ s,
- Fast semiconductor fuses: they are installed in DC-link and AC terminals of power inverter,**
- 2) A circuit breaker: installed in output terminal of inverter after the LC filter and before connecting to the grid or local load,
- 3) Short-circuit protection system of IPM: IPMs are commonly equipped by an inner protection system against short-circuit, under-voltage of module's power supply, and over-temperature fault in module.

Up to now all the aforementioned above designed protection systems have worked several times and prepared a safe operation condition for the inverter against severe short-circuit or over-current faults.

### Overvoltage

Transient overvoltage due to switching and leakage inductance is the common source of overvoltage in power electronics converter. Snubber circuits and transient voltage suppressors like BOD, MOV and TVS diodes are the remarkable protection methods. In present studied application, snubber circuits (C type) and MOV protection methods are used to protect power inverter modules against any probable transient over-voltages. Up to know this protection system has worked at least two times, both when a short circuit fault has been happened incidentally by the output local AC load and as a result a transient overvoltage due to abrupt change in output current and DC-link leakage inductance is occurred.

Steady-state overvoltage may occur at input DC-link or output AC inverter's terminals. In this case, it is recommended to trip the power electronics converter and inform operator to remove the fault. To do this a PLC or microcontroller such as DSP can monitor the system and inform operator in the case of overvoltage fault condition.

DC over/under voltage protection monitors dc link voltage and turn off IGBT switches consequential a fault. Since electronic systems, micro controller, IGBT drivers and so on are often supplied through dc link; it is necessary to consider dc-link under voltage protection.

A summary of protection system is shown in Fig. 7. Almost all protections are done in DSP; backup hardware protection is also included to ensure the highest protection level. As the most

effective protection strategy, all switches are turned off after fault detection by protection system.

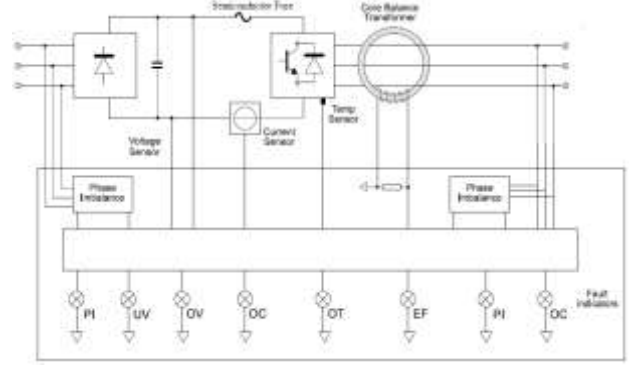


**Figure 7. protection system**

### LCL Filter Design

Fig. 2 shows the system topology of 85-kVA grid-tied AC/DC/AC converter for the microturbine-based power generation system. In this converter an LCL filter is used to connect the inverter output with the grid.

The LCL filter generally is used to decrease the switching ripple. In fact, compared with the L filter, an LCL filter with only a small increase in filter hardware could decrease the switching ripple adequately, and its components could be characterized as the following:

$$Z_I = R_I + L_I s \quad (4)$$

$$Z_G = (R_G + R_S) + (L_G + L_S) s \quad (5)$$

$$Z_O = R_D + \frac{1}{C_F s} \quad (6)$$

Here,  $L_I$  and  $R_I$  are the inverter-side inductance and its equivalent series resistor (ESR), respectively;  $L_G$  and  $R_G$  are the grid-side inductance and its ESR;  $L_S$  and  $R_S$  are the equivalent series inductance and resistor (impedance) of the source.  $C_F$  is the capacitance of the LCL filter which is in series with  $R_D$ , the damping resistor of the LCL filter.

Three transfer functions related to the LCL filter that are useful to design filter's different parameters and also adjust inverter's current controller, are given as

$$G_{V_i I_1}(s) = \frac{I_1(s)}{V_i(s)} = \frac{Z_o + Z_g}{Z_i Z_g + Z_g Z_o + Z_o Z_i} \quad (7)$$

$$G_{V_i I_2}(s) = \frac{I_2(s)}{V_i(s)} = \frac{Z_o}{Z_i Z_g + Z_g Z_o + Z_o Z_i} \quad (8)$$

$$G_{I_1 I_2}(s) = \frac{I_2(s)}{I_1(s)} = \frac{G_{V_i I_2}(s)}{G_{V_i I_1}(s)} = \frac{Z_o}{Z_o + Z_g} \quad (9)$$

Here,  $I_1(s)$  and  $I_2(s)$  are the inverter output current and the grid-side current, and  $V_i(s)$  is the voltage generated by the inverter at its terminals.

The following design considerations are taken into account to determine the LCL filter parameters:

- 1) The selection of the ripple current is a trade-off among inductor  $L_I$  size, IGBT switching and conduction losses, and inductor coil and core losses. The smaller the ripple current, the lower the IGBT switching and conduction losses, but the larger the inductor, resulting in larger coil and core losses. Typically, the ripple current can be chosen as 15%-35% of rated current. For this case, the ripple current is selected as 33.5% of the rated current. The maximum current ripple can be derived as in (10) [27]:

$$\Delta i_{L_I, \max} = \frac{1}{8} \cdot \frac{V_{dc}}{L_I \cdot f_{SW}} = 33.5\% \cdot i_{rated} \quad (10)$$

- 2) The selection of the capacitor is a trade-off between reactive power in  $C_F$  and  $L_I$  inductance. The more capacitance, the more

reactive power flowing into the capacitor, and the more current demand from the  $L_1$  and the switches. As a result, the efficiency will be lower. The capacitance cannot be too small either. Otherwise, the inductance will be large in order to meet the attenuation requirements. The larger inductance  $L_1$  resulted from smaller capacitance leads to higher voltage drop across the inductor  $L_1$ . In this design, the reactive power is chosen as 15% of the rated power [27].

$$C_F = 15\% \cdot \frac{P_{rated}}{2\pi f_{Line} \cdot V_{LL}^2} \quad (11)$$

3) The resonance frequency should be included in a range between ten times the line frequency and one half of the switching frequency in order not to create resonance problems in the lower and higher parts of the harmonic spectrum. The passive resistors should be chosen as a compromise between the necessary damping and the losses in the system [28].

$$f_{res} \cong \frac{1}{2\pi} \sqrt{\frac{L_i + L_g}{L_i L_g C_F}} \quad (12)$$

4) Passive damping must be sufficient to avoid oscillation, but losses cannot be so high as to reduce efficiency [28].

$$R_D = 50\% \times \frac{1}{2\pi f_{res} \cdot C_F} \quad (13)$$

Table I shows the system parameters.

Fig. 8 shows the magnitude plot of the LCL filter transfer functions. As it could be seen from this figure the filter in the low-frequency range (below resonant frequency) can be approximated as the sum of the overall inductance ( $L_1+L_G+L_S$ ); and in the high frequency range, as the inverter side inductor alone ( $L_1$ ). It is assumed that at high frequencies, the capacitor acts as a short circuit.

**Controller Design**

Power electronic interface should be operated in stand alone and grid connected mode. System model with designed parameters are used to design the system controller. Here, control approach at both operation modes is done.

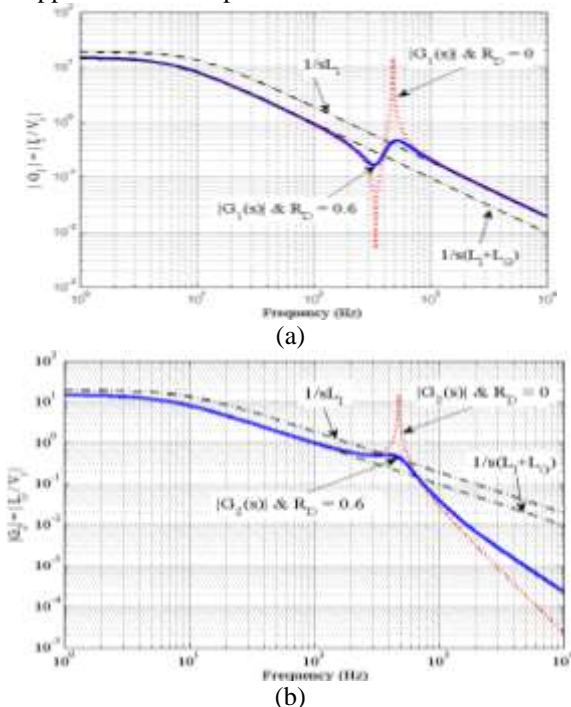


Figure 8. LCL filter forward admittance transfer function magnitude plots versus frequency; (a) forward self-admittance transfer function  $G_1(s)$ ; (b) forward trans-admittance  $G_2(s)$

**Current controller design at grid connected mode**

Fig. 5 shows the single phase equivalent circuit of the grid connected inverter to design linear controller; switch S status determines whether system is operated at off grid mode or grid tied mode. Where LCL parameters are as:  $L_1=0.9$  mH,  $L_g=1$  mH,  $C_f=84$   $\mu$ F,  $R_d=2.1$   $\Omega$  and  $Z_L=8$ .

Controller circuit is designed to control inverter at grid connected and stand alone modes. The standard PI controller with feedback control mode is used; as shown in Fig. 10,  $U_g$  (grid voltage feed-forward) is an input disturbance. Control method aims to produce the suitable inverter output voltage so that inverter output current is regulated. As a result, required active and reactive power is delivered to grid [11].

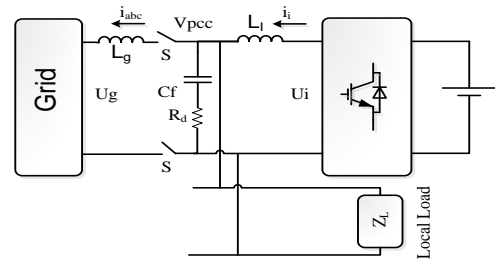


Figure 9. Single phase equivalent circuit of the grid connected inverter

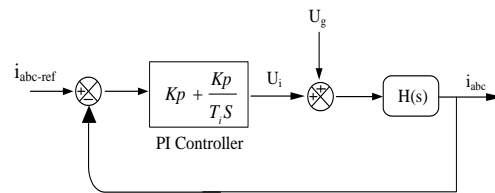


Figure 10. PI controller scheme at grid connected mode PI controller is designed as:

$$G_{PI}(S) = Kp + \frac{K_I}{S} \quad (14)$$

The plant transfer function in terms of inverter output voltage and current is defined as [11]:

$$H_f(S) = \frac{i_i(S)}{U_i(S)} = \frac{L_1 C_f S^2 + R_D C_f S + 1}{L_1 L_g C_f S^3 + (R_D L_1 C_f + R_D L_g C_f) S^2 + (L_1 + L_g) S} \quad (15)$$

Fig. 11 shows pole-zero plot of open loop system. There are two complex and one real pole.

Steady state errors and dynamic criteria are used to design integrator gain K. Proportional gain is chosen 4 to achieve damping value  $\zeta=0.7$ . The integrator time constant  $T_i$  was chosen 9 millisecond as a compromise between noise cancellation and system dynamic.

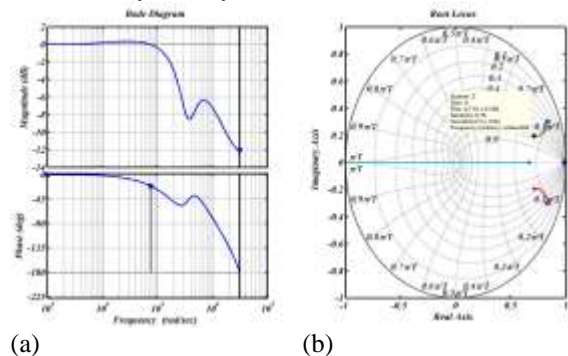


Figure 11. System plots of closed loop system in grid connected mode (a) root-locus map (b) the bode plot Voltage controller design in stand alone mode

The control scheme is shown in Fig. 12. Inverter output voltage is used in closed loop system.

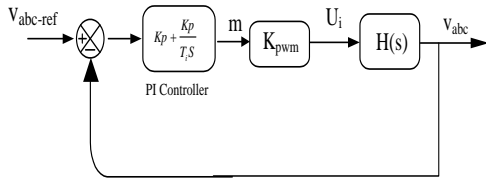


Figure 12. Control scheme in stand-alone mode

Where plant transfer function  $H(S)$  is defined in terms of load voltage  $V_{pcc}$  and inverter output voltage  $U_i$ ;  $Z_L$  is the load equivalent impedance [11].

$$H(S) = \frac{v_{pcc}(S)}{U_i(S)} = \frac{R_D Z_G C_F S + Z_G}{L_1 L_G C_F S^3 + (R_D + Z_G) L_1 C_F + R_D L_G C_F S^2 + (L_1 + L_G + R_D Z_G C_F) S + Z_G} \quad (16)$$

$K_p=0.08$  and  $K_i=0.0002$  are determined as optimal parameters. Fig. 13 (a) and (b) show the zero-pole placement at the open-loop and closed loop system plot. Damping factor is 1 at dominant pole and overshoot is negligible. Closed loop system is stable as well.

EXPERIMENTAL RESULTS

The constructed inverter is tested under different load and grid scenarios. A photograph of constructed setup is shown in Fig. 14. First, islanding operation of inverter is evaluated. Fig. 15 shows the experimental results of this test. In Figs. 15(a) and (d) the reference voltage in  $d$ -axis,  $V_{d-ref}$ , is changed from a positive value to a negative value with a similar amplitude but different sign. It means that the voltage amplitude always remain constant but the voltage phase suddenly changed by a  $180^\circ$  step. Figs. 15 (b-c) and 6 (e-f) are demonstrated the experimental results of islanding operation when the reference voltage is changed between two different constant values. Experimental results shows the inverter have a good performance in the stand-alone mode of operation.

Second test scenario is the seamless transfer process between two control modes. Figs 16(a) and (d) shows first step of seamless transfer process described in section III-C-1. In these Figs. the bottom waveform is the phase difference between voltages at the PCC and the grid, named  $\Delta\theta_{PG}$ . Fig. 16(b) demonstrates one step of seamless transfer process. The fourth waveform,  $C_{SG}$ , shows a criterion variable that DSP evaluates the seamless transfer before sending a closing command to the relay  $K$ . Also, the third waveform shows the feedback signals that relay  $K$  send back to the DSP and shows the present statuses of relay. Fig. 16(e) shows the output signal of PLL that is the voltage phase in grid side. Figs. 16(c) and (f) show waveforms of the voltage and the current of inverter and grid when transferring between different modes are under processing.

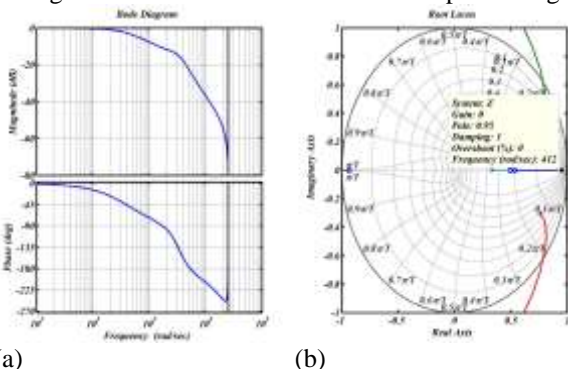
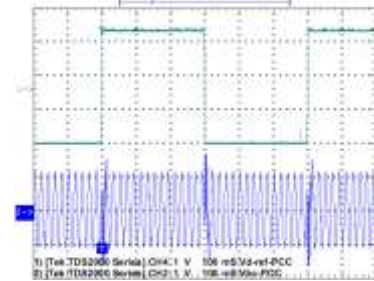


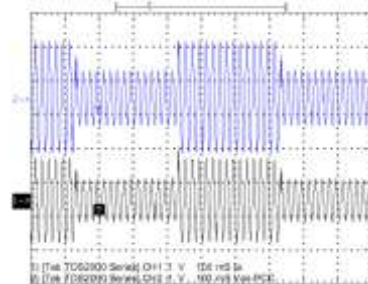
Figure 13. Plots of closed-loop system in stand-alone mode (a) root-locus map (b) the bode plot Open-loop



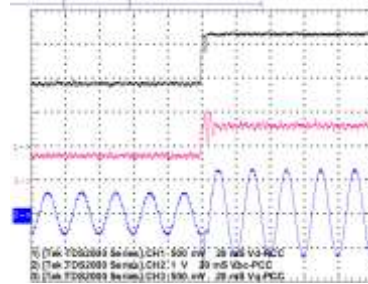
Figure 14. Photograph of constructed DC/AC converter.



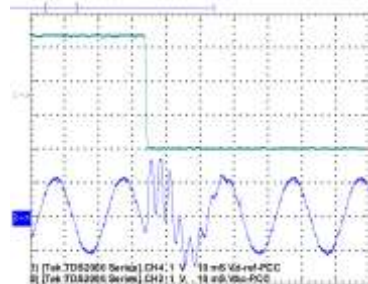
(a)



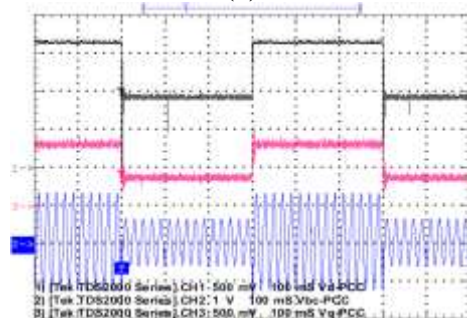
(b)



(c)



(d)



(e)

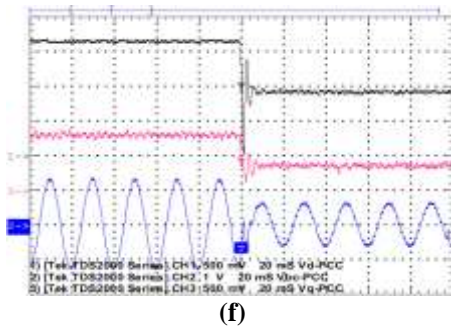


Figure 15. Experimental results when the inverter works in stand-alone mode: waveforms from top to bottom are (a, and d)  $v_{d-ref}$  &  $v_{ab-pcc}$ ; (b)  $v_{ab-pcc}$  &  $i_a$ ; (c, e, and f)  $v_{d-pcc}$  &  $v_{q-pcc}$  &  $v_{ab-pcc}$ .

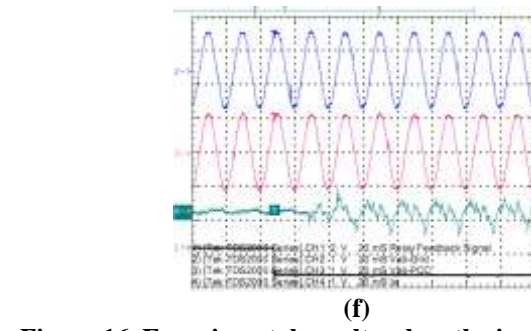
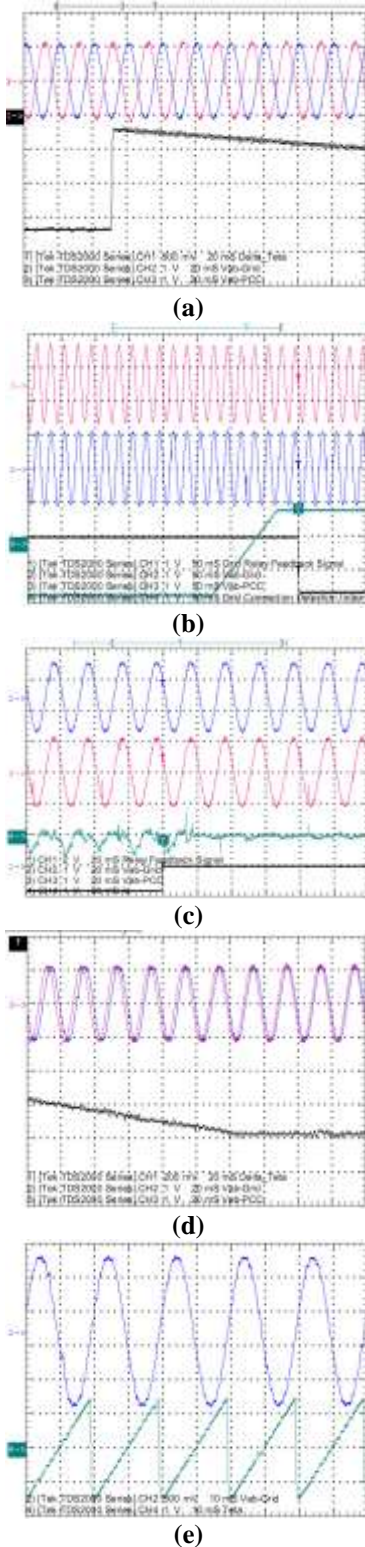


Figure 16. Experimental results when the inverter works in seamless transfer process: waveforms from top to bottom are (a, and d)  $V_{ab-PCC}$ ,  $V_{ab-grid}$  &  $\Delta\theta_{PG}$ ; (b)  $V_{ab-grid}$  &  $V_{ab-PCC}$  &  $S_{FR}$  &  $C_{SG}$ ; (c, and f)  $V_{ab-grid}$  &  $V_{ab-PCC}$  &  $i_a$  &  $S_{FR}$ ; (e)  $V_{ab-grid}$  &  $\theta_{PLL}$ .

Experimental results related to the grid-connected control mode are depicted in Fig. 17. The grid voltage and inverter current waveforms are shown in Figs. 17(a) and (b) when the reference active and reactive power is changed from zero (in Fig. 17(a)) to 5-kW & 2-kVAr (in Fig 17(b)). The output current of inverter, as shown in Fig. 17(b), is highly distorted. The main reason for this current distortion is the grid voltage that has 3% of 5th harmonic and 1.5% of unbalanced voltage. Fig. 17(c) shows the inverter related voltage and current waveforms under an over-current fault condition. In this test two voltage phases in grid side are replaced and then a command of connecting to the grid has been sent to the DSP controller. As shown in the Fig. 17(c), the software protection system is acted immediately and sent opening command to the relay  $K$  (fourth waveform,  $S_{DR}$ ) but electromechanical relay  $K$  needs 45-ms time to be opened. During this time, a set of current is flown from grid toward the filter capacitance bank.

CONCLUSION

Inverter is an important part of a microturbine-based distribution generation system. In this paper, a DSP-based digital controller in order to control a three-phase inverter in stand-alone and grid-connected modes is studied. The three-phase inverter, in fact, is a three-leg power converter which is switched in 2-kHz frequency by the controller with a sinusoidal PWM pattern. An 85-kVA three-phase inverter setup is developed and tested under different source and load scenarios. Experimental results prove the effectiveness and appropriate operation of designed controller. Based on experimental results in stand-alone control mode, output voltages are sinusoidal and balanced only with a low distortion level (voltage THD is less than 3%). In grid-connected control mode, distortion on grid voltage results a distorted inverter output current. To compensate this distortion, a harmonics suppression control block must be added to the inverter controller. The experimental results show that seamless transfer between two modes has been achieved well, but because of polluted grid voltage, waveform quality of the grid current is not good

REFERENCES

- [1] F. S. Pai, and S. J. Huang, "Design and Operation of Power Converter for Microturbine Powered Distributed Generator with Capacity Expansion Capability," IEEE Trans. Energy Conversion, vol. 23, no. 1, pp. 110-118, March 2008.
- [2] H. K. Karegar, and A. Shabani, "Effects of Inverter Modulation Index on the Stability of Grid Connected Micro-Turbines," in Proc. 2nd IEEE Conf. on Power and Energy (PECon 08), pp. 1623-1627, Dec. 2008.
- [3] M. S. Rho, G. R. Kim, Y. K. Choi, and M. S. Chae, "Development of Power Conditioning System for a Microturbine in Vehicle," in Proc. IEEE Power Electron. Spec. Conf. (PESC 2007), pp. 1496-1501, Jun. 2007.

- [4] Z. Ye, T. C. Y. Wang, G. Sinha, and R. Zhang, "Efficiency Comparison for Microturbine Power Conditioning Systems," in Proc. 34th IEEE Annu. Power Electron. Spec. Conf. (PESC [17] T. Kerekes, R. Teodorescu, M. Liserre, C. Klumpner, and M. Summer, "Evaluation of Three-Phase Transformerless [18] Photovoltaic Inverter Topologies," IEEE Trans. Power Electronics, vol. 24, no. 9, pp. 2202-2211, Sep. 2009.
- [5] H. Bai, F. Wang, D. Wang, C. L. Liu, and T.Y. Wang, "A Pole Assignment of State Feedback based on System Matrix for Three-Phase Four-Leg Inverter of High Speed PM Generator Driven by Micro-Turbine," in Proc. 4th IEEE Conf. Ind. Electron. and Appl. (ICIEA 2009), pp. 1361-1366, May 2009.
- [6] Z. Yunhai, and J. Stenzel, "Simulation of a Microturbine Generation System for Grid Connected and Islanding Operations," in Proc. Asia-Pacific Power and Energy Eng. Conf. (APPEEC 2009), pp. 1-5, March 2009.
- [7] T. C. Green, and M. Prodanović, "Control of Inverter-Based Micro-Grids," Elec. Power Sys. Res., pp. 1204-1213, 2007.
- [8] M. N. Marwali, and A. Keyhani, "Control of Distributed Generation Systems—Part I: Voltages and Currents Control," IEEE Trans. Power Electron., vol. 19, no. 6, pp.1541-1550, Nov. 2004.
- [9] L. Asiminoaei, R. Teodorescu, F. Blaabjerg, and U. Borup, "A Digital Controlled PV-Inverter with Grid Impedance Estimation for ENS Detection," IEEE Trans. Power Electron., vol. 20, no. 6, pp.1480-1490, Nov. 2005.
- [10] IEEE Recommended Practices and Requirements for Harmonic Control in Electrical Power systems, IEEE Std. 519-1992, 1992.
- [11] R. Teodorescu, and F. Blaabjerg, "Flexible Control of Small Wind Turbines with Grid Failure Detection Operation in Stand-Alone and Grid-Connected Mode," IEEE Trans. Power Electron., vol. 19, no. 5, pp.1323-1332, Sep. 2004.
- [12] G. Shen, D. Xu, L. Cao, and X. Zhu, "An Improved Control Strategy for Grid-Connected Voltage Source Inverters with an LCL Filter," IEEE Trans. Power Electron., vol. 23, no. 4, pp. 1899-1906, July 2008.
- [13] M. Ciobotaru, V. G. Agelidis, R. Teodorescu, and F. Blaabjerg, "Accurate and Less-Disturbing Active Antiislanding Method Based on PLL for Grid-Connected Converters," IEEE Trans. Power Electron., vol. 25, no. 6, pp. 1576-1584, June 2010.
- [14] R. Tirumala, N. Mohan, and C. Henze, "Seamless Transfer of Grid-Connected PWM Inverters Between Utility-Interactive and Stand-Alone Modes," in Proc. IEEE Appl. Power Electron. Conf., pp. 1081–1086, 2002.
- [15] Z. Yao, L. Xiao, and Y. Yan, "Seamless Transfer of Single-Phase Grid-Interactive Inverters Between Grid-Connected and Stand-Alone Modes," IEEE Trans. Power Electron., vol. 25, no. 6, pp. 1597-1603, June 2010.
- [16] H. G. Jeong, K. B. Lee, S. Choi, and W. Choi, "Performance Improvement of LCL-Filter-Based Grid-Connected Inverters Using PQR Power Transformation," IEEE Trans. Power Electron., vol. 25, no. 5, pp. 1320-1330, May 2010.
- [17] T. Kerekes, R. Teodorescu, M. Liserre, C. Klumpner, and M. Summer, "Evaluation of Three-Phase Transformerless [18] Photovoltaic Inverter Topologies," IEEE Trans. Power Electronics, vol. 24, no. 9, pp. 2202-2211, Sep. 2009.
- [19] J. Gabe, V. F. Montagner, and H. Pinheiro, "Design and Implementation of a Robust Current Controller for VSI Connected to the Grid Through an LCL Filter," IEEE Trans. Power Electron., vol. 24, n0. 6, pp. 1444-1452, June 2009.
- [20] H. L. Jou, W. J. Chiang, and J. C. Wu, "A Simplified Control Method for the Grid-Connected Inverter With the Function of Islanding Detection," IEEE Trans. Power Electron., vol. 23, no. 6, pp. 2775-2783, Nov. 2008.
- [21] Y. A. R. I. Mohamed, and E. F. E. Saadany, "Hybrid Variable-Structure Control With Evolutionary Optimum-Tuning Algorithm for Fast Grid-Voltage Regulation Using Inverter-Based," IEEE Trans. Power Electron., vol. 23, no. 3, pp. 1334-1341, May 2008.
- [22] S. Y. Park, C. L. Chen, J. S. Lai, and S. R. Moon, "Admittance Compensation in Current Loop Control for a Grid-Tie LCL Fuel Cell Inverter," IEEE Trans. Power Electron., vol. 23, no. 4, pp. 1716-1723, July 2008.
- [23] M. Dai, M. N. Marwali, J. W. Jung, and A. Keyhani, "Power Flow Control of a Single Distributed Generation Unit," IEEE Trans. Power Electron., vol. 23, no. 1, pp. 343-352, Jan. 2008.
- [24] M. Castilla, J. Miret, J. Sosa, J. Matas, L. G. D. Vicuña, "Grid Fault Control Scheme for Three-Phase Photovoltaic Inverters with Adjustable Power Quality Characteristics," IEEE Trans. Power Electron., Early Access, 2010.
- [25] X. Wang, X. Ruan, S. Liu, and C. K. Tse, "Full Feed-Forward of Grid Voltage for Grid-Connected Inverter with LCL Filter to Suppress Current Distortion Due to Grid Voltage Harmonics," IEEE Trans. Power Electron., Early Access, 2010.
- [26] T. Abeyasekera, C. M. Johnson, D. J. Atkinson, and M. Armstrong, "Suppression of Line Voltage Related Distortion in Current Controlled Grid Connected Inverters," IEEE Trans. Power Electron., vol. 20, no. 6, pp- 1393-1401, Nov. 2005.
- [27] T. Hornik, and Q. C. Zhong, "A Current Control Strategy for Voltage-Source Inverters in Microgrids," IEEE Trans. Power Electron., Early Access, 2010.
- [28] T. C. Wang, Z. Ye, G. Sinha, and X. Yuan, "Output Filter Design for a Grid-Interconnected Three-Phase Inverter," in Proc. IEEE Conf., 2003.
- [29] M. Liserre, F. Blaabjerg, and S. Hansen, "Design and Control of an LCL-Filter-Based Three-Phase Active Rectifier," IEEE Trans. Ind. Applic., vol. 41, no. 5, Sep./Oct. 2005.